Constraints on transport and superconductivity in quantum matter

Debanjan Chowdhury

E-mail: debanjanchowdhury@cornell.edu Department of Physics, Cornell University, Ithaca NY-14853, USA

Abstract. Transport and superconductivity in weakly interacting metals are governed by the long-lived quasiparticles near sharp electronic Fermi surfaces. Motivated by empirical evidence for seemingly universal quantum bounds on transport scattering rates and superconducting transition temperatures across strongly correlated metals, I discuss "solvable" examples of correlated fermionic systems that provide unique insights into these puzzling phenomena. In the first part, I survey a few distinct examples of metallic phases exhibiting T-linear resistivity above a characteristic temperature T^* , and discuss possible implications on transport bounds. In the second part, I demonstrate how to formulate rigorous bounds on T_c for two-dimensional superconductors in the absence of a microscopic theory of superconductivity. The examples raise fundamental questions about bounds in quantum many-body systems that can provide new perspectives on unconventional transport and high-temperature superconductivity in correlated electronic solids.

Please send me an email if you spot any typos and notice important missing citations.

Contents

1	Intr	roduction	2
2	Quantum bounds on transport and superconductivity?		4
3	A brief survey of IR-incomplete non-Fermi liquids		7
	3.1	Electron-phonon scattering in equipartition regime	8
	3.2	Hot quantum matter in ultracold atom simulators	9
	3.3	Charge frustrated bad metals	11
	3.4	Bottom-up approach: Planckian transport in magnetic delafossites	14
4	Superconductivity is not boundless		18
	4.1	Raising T_c — an optimization problem	19
	4.2	Revisiting upper bounds on $T_c/D_s(0)$	21
	4.3	Fundamental upper bounds from optical sum-rules	22
5 Outlook		25	

1. Introduction

The investigation of electron propagation through quantum materials in response to weak electric fields has been central to both experimental and theoretical condensed matter and materials physics research for over a century. Nearly all major discoveries in condensed matter physics — from superconductivity to the quantum Hall effect —have relied on measuring dc electrical transport properties of materials. Low-temperature transport studies enable bridging macroscopic material properties, namely electrical conductivity, with the quantum mechanical properties of the interacting many-electron Hamiltonian through its ground state and low-lying excitations in quantum solids. However, for strongly correlated metals, it has been aptly observed that "... dc transport is the first thing one measures, and the last thing one understands." * The theoretical description of transport in real materials presents a two-fold challenge: First, constructing a minimal model that incorporates all "relevant" degrees of freedom responsible for scattering is formidable — electrons scatter off nearly everything in electronic solids. Second, even with a well-understood microscopic model, reliably "solving" it, especially in the regime of strong interactions, to extract transport coefficients can be even more challenging.

In the first part of these lectures, we will focus on transport in quasi-two-dimensional systems, where resistivity is measured in units of $R_Q = h/e^2$ † In the absence of any microscopic theory of transport, one can speculate that the longitudinal resistivity takes the form:

$$\frac{\rho}{R_Q} = \rho \left(\left\{ \frac{T}{T^*} \right\}, \frac{\ell}{a}, \frac{Ba^2}{\Phi_0}, \dots \right), \tag{1}$$

where T^* are characteristic temperature scales associated with the metal (e.g., Fermi temperature, renormalized bandwidth, Bloch-Grüneissen temperature, etc.), ℓ is a characteristic length scale determined by disorder and/or interaction-induced mean-free path relative to a microscopic length scale (e.g., lattice constant or Bohr radius), Ba^2 is the magnetic flux relative to the flux quantum Φ_0 , and so on. When $T \to 0$ and in exceptionally clean samples (i.e., in the absence of elastic scattering off impurities), $\rho \to 0$ in a translationally invariant metal and $\rho \to \infty$ in an insulator. ‡ Generically, one might expect $\rho \sim O(R_Q)$ otherwise, as this is the only natural scale in the problem. However, in "good" metals with a long mean-free path $(k_F \ell \gg 1)$, $\rho \ll R_Q$; we will address a puzzle inspired by experiments in a real material that is a good metal, but where the T-dependence of the resistivity is quite intriguing and raises a number of interesting questions. In these lectures, we will be interested in the temperature evolution of resistivity, $\rho(T)$, which in an ideal scenario can be backtracked to infer the dominant scattering source for the electrons. For instance, in the vast majority of "conventional" metals, the T-dependence of resistivity is dominated by electron-phonon

^{*}This quote has been attributed to a number of condensed matter experimentalists.

[†]In d-dimensions, this is instead $R_Q = (h/e^2)[a]^{d-2}$.

 $^{^{\}ddagger}$ Of course, $\rho = 0$ also in a superconductor regardless of these caveats, below the transition temperature.

scattering, which is T-linear above a characteristic temperature scale, crossing over to a power-law T^{d+2} below that scale [1]. *

Our interest in these lectures will be on "unconventional" regimes of metallic behavior, both of the "good" and "bad" variety, where the latter are characterized by a short mean-free path $(k_F \ell \sim 1)$ and $\rho \gtrsim R_Q$. Transport in bad metals cannot be understood in terms of any standard paradigm of scattering of long-lived quasiparticles with long mean-free paths [2]. We shall be particularly interested in metals where $\rho(T) = \rho_0 + AT$, the problem of so-called "T-linear resistivity," inspired in part by the ubiquity of this phenomenon [3]. Of course, such behavior is not necessarily a sign of unconventional behavior since most conventional metals exhibit T-linear resistivity at intermediate (and room) temperatures due to electron-phonon scattering. Our focus here will be on theoretical mechanisms that are not of this type, and on materials where it is not a priori obvious that phonons are solely responsible for the observed T-linearity. Unfortunately, building a quantitative theory of transport from first principles for materials can be quite challenging, since there is often no systematic method to disentangle the effects of electron-electron and electron-phonon interactions in an obvious fashion, as well as the contribution due to various forms of inhomogeneities that are inevitably present spanning length scales. We will keep returning to various elements of this interesting problem during the course of the first lecture.

The other quantum mechanical phenomenon that has captivated physicists since its discovery is superconductivity, and it is safe to say that nearly all experimental discoveries have been serendipitous. From a theoretical perspective, making predictions for either the superconducting transition temperature T_c (and relatedly the mechanism) is a notoriously difficult problem. Once again, the challenges are two-fold: First, building an accurate microscopic model that incorporates the key material properties that fundamentally control T_c in an electronic solid. This is an issue even in "conventional" superconductors where the Bardeen-Cooper-Schrieffer (BCS) theory, and its various extensions, can be applied. Second, even when the starting microscopic model is well understood and in the intermediate to strong-coupling regime (i.e., outside the regime of validity of any weak-coupling BCS-like approach), a "controlled" theory for superconductivity is typically unavailable.

In analogy with Eq. (1), and in the absence of a microscopic theory for T_c , one naively expects it to depend on the effective electron-electron and electron-phonon interactions, some basic properties of the quantum-mechanical electronic wavefunctions, on the nature of disorder, and so on. While there has been a great deal of progress in combining first-principles-based computations with fully self-consistent Migdal-Eliashberg theory, our interest here will be on formulating some general principles on how to make concrete statements about the microscopic factors that fundamentally limit T_c in regimes where the above approaches do not necessarily work. In the second part of these lectures, we will focus specifically on two-dimensional systems and scrutinize

^{*}In most metals that are not "ultra-clean", one does not encounter the phenomenon of "phonon-drag".

what energy scales associated with sufficiently generic models of correlated electronic solids must fundamentally limit T_c from above. Importantly, the goal here will not be to predict T_c or propose new mechanisms for superconductivity, but instead motivate how one might be able to put strong constraints on how high T_c can be in principle without any knowledge of the properties of the potential superconducting phase. We will begin by demonstrating via explicit examples how many of the physically relevant quantities that are widely believed to serve as (heuristic) upper bounds on T_c are not fundamental upper bounds. We will then end by formulating rigorous upper bounds on T_c by leveraging the power of optical sum-rules, which will also have some connections to our previous discussion of transport.

The following material is primarily pedagogical and based on two lectures delivered by the author at the Boulder Summer School for Condensed Matter and Materials Physics on the Dynamics of Correlated Electrons. The remainder of this article is organized as follows: In Sec. 2, based on a large body of experimental work, we make the case that in the regime of strong interactions, there are potentially quite general and "universal" bounds that characterize both transport scattering rates and superconducting T_c 's regardless of microscopic details, and critically examine these possibilities using different perspectives in subsequent sections. In Sec. 3 we discuss a variety of examples of unconventional metallic transport, including T-linear resistivity, and place them in the context of our discussion on bounds on scattering rates. Addressing these examples brings out a number of new and interesting questions that deserve careful future study. In Sec. 4 we turn to the question of what energy scales do not fundamentally limit T_c , and instead best serve as "heuristic" upper bounds, in the absence of a microscopic starting point; we end by formulating how to rigorously bound T_c using optical sum-rules.

2. Quantum bounds on transport and superconductivity?

The study of electrical transport in interacting metals has a long and distinguished history that predates the development of quantum mechanics. This journey traces back to 1900, when Paul Drude related the motion of conduction electrons in metals —albeit as a classical gas of free particles — to conductivity and Ohm's law by introducing the concept of a phenomenological electron momentum relaxation rate, or equivalently, an inverse collision time (τ) [4]. He wrote down Newton's equation of motion for individual electronic momenta: $d\mathbf{p}/dt = -\mathbf{p}/\tau + \mathbf{F}$, where t is time and \mathbf{F} is the external force. Despite its simplicity and non-universal phenomenological nature, this ultimately also leads to some basic understanding of the electrical conductivity at a finite frequency, $\sigma(\omega) = \sigma_0/(1-i\omega\tau)$. Here, σ_0 depends on material parameters such as electron density, electron charge, effective mass, and τ . In the original treatment, the source of momentum relaxation was assumed to be due to the inevitable presence of random impurities, which serves as a source of elastic scattering, leading to a residual resistivity in the zero-temperature limit. In what follows, and in most of the present-day

discussion of electrical transport in highly correlated metals, we focus on the inelastic scattering mechanisms that control the temperature dependence of dc resistivity and $\tau(T)$, even when the Drude model itself might not be an accurate description of the microscopic theory.

Since carrier densities and effective masses can vary dramatically between different materials, direct comparisons of resistivity values across various substances often lack meaningful interpretation. A more illuminating approach involves examining the possibly "universal" relaxation timescales that characterize transport phenomena. However, extracting transport scattering rate $\Gamma(=\tau^{-1})$ from dc resistivity measurements presents significant challenges. Ideally, Γ is best extracted from optical conductivity measurements, for instance from the "width" of the Drude-like peak [5]. However, in many materials of interest, this is not possible and so an alternative methodology has been used to extract the temperature-dependent Γ [3] that employs a Drude fitting approach. The simplest approach is to express $\rho = m_{\star} \Gamma / n_c e^2$, where m_{\star} is an effective mass (often extracted from quantum oscillations or specific heat measurements) and n_c is the effective carrier density (typically extracted from Hall or quantum oscillation measurements). In materials with complex fermiology and anisotropic Fermi velocities, the above approximations need to be carefully scrutinized. * By further assuming that m_{\star} and n_c remain temperature-independent [†] and focusing only on the inelastic part of the dc resistivity, $\rho - \rho_0 = AT$, this yields:

$$\Gamma \equiv \alpha \frac{k_B T}{\hbar}, \quad \alpha = \frac{\hbar}{k_B} \frac{e^2 n_c}{m_+} A.$$
 (2)

See Refs. [7, 8] for a more in-depth discussion of some of the caveats and challenges associated with this protocol. Despite some of the inherent uncertainties, it is striking that numerous correlated metals, e.g. the cuprates, pnictides, ruthenates, organics, and rare-earth element based compounds, displaying T-linear resistivity with a finite A-coefficient yield $\alpha \approx O(1)$ with the above "operational" definition of a transport scattering rate [3, 9]. More recently, the same analysis has also been applied to transport data in magic-angle twisted bilayer graphene (MATBG) near half-filling of the electron and hole-like flat-bands [10] where $\alpha \sim O(1)$, and contrasted against older data in monolayer graphene [11, 12] where $\alpha \sim 10^{-2}$. The observation of a T-linear resistivity accompanied by a scattering rate with $\alpha \sim O(1)$ is commonly referred to as "Planckian" scattering [13, 14]. Of course, as discussed in Sec. 1 and was noted by Peierls in 1934 [15], electron-phonon scattering above a characteristic temperature yields Planckian scattering rates of the form in Eq. (2). Moreover, a similar Drude-analysis leads to $\alpha \sim O(1)$ in many conventional metals (e.g. Cu, Au, Al, etc.).

However, one of the most striking aspects of the above analysis is the presence of a single regime of T-linear resistivity over an extended temperature range, at least in some parameter regimes (e.g., in optimally doped cuprates [16] and over a range of

^{*}See supplementary material of Ref. [3] for the analysis in multi-orbital systems.

[†]See a recent optical conductivity analysis [6], which concludes that an effective T-dependent m_{\star} conspires with a conventional $\Gamma(T)$ to yield a T-linear resistivity in a specific compound (CeCoIn₅).

fillings in MATBG [17]), where the A coefficient is constant and the scattering rate is Planckian. This is surprising because in materials with complex unit cells that host multiple optical phonon branches (see e.g. [18, 19] for discussion of phonons in these materials), if the electrons scatter off these phonons with increasing temperature, one would naively expect based on Matthiessen's rule that there would be a sequence of smooth crossovers leading to deviations from a single regime of T-linear resistivity. * This observation has inspired one of the central questions and the Planckian "conjecture in the field †: Is there a fundamental bound on how large the inelastic transport scattering rate can be in a generic correlated electronic system?

Part of the interest in correlated metals with seemingly "universal" Planckian scattering rates is that a large fraction of them (e.g., cuprates, pnictides, ruthenates, heavy-fermion compounds, organics, MATBG and so on) are also "high" temperature superconductors with a largely unknown pairing mechanism. However, this statement requires immediate scrutiny—how do we quantify "high"? While for practical applications one might be interested in the absolute value of T_c , as theorists we are typically interested in T_c relative to some intrinsic energy scales associated with the material. In that sense, many heavy-fermion and moir superconductors with a relatively "low" absolute value of T_c are still considered to be "high" temperature superconductors. Unfortunately, it is typically not immediately clear which of the microscopic energy scales in a material directly influence T_c , or its maximum possible value. In the absence of any fundamental understanding of these issues, one can once again turn to empirical observations. In this regard, one of the most striking trends in T_c in correlated systems was systematically analyzed and pointed out by Uemura and collaborators [22]. By examining the ratio of T_c/T_F , where T_F represents a "proxy" for a Fermi temperature in the parent metallic state, they observed that various unconventional superconductors (including hole-doped cuprates as a function of underdoping) have relatively "large" values of $T_c/T_F \approx 10^{-2}$. More recently, twisted multilayer graphene superconductors with partially filled nearly flat bands demonstrate an even higher ratio of $T_c/T_F \approx 10^{-1}$ [23]. Importantly, such behavior is unexpected in the standard BCS-like regime of conventional superconductors. Indeed, elemental metals (e.g. Al, Sn, Zn) exhibit much smaller ratios of $T_c/T_F \approx 10^{-4}$. Thus, empirically strongly correlated superconductors appear to show values of T_c that are much closer to T_F compared to their weakly correlated counterparts. Of course, given the observed Planckian scattering rates in the normal state and the relatively large ratios of T_c/T_F across many of these systems, one might wonder if there exist any fundamental close connections between the two phenomena. This remains an open question at the moment.

However, there are several intriguing aspects associated with these observations. First, accurately determining T_F from experiments can present significant challenges.

^{*}In overdoped cuprates, it has been suggested that the slope does change and the higher-temperature T-linear resistivity might arise from electron-phonon scattering [20].

[†]Unfortunately, there is no "universal" definition for a transport scattering rate, which complicates the formulation of precise (conjectured) Planckian bounds [21].

The process often relies on measuring n_c and m_{\star} through a combination of Hall measurements and quantum oscillations, and then using the standard expression for T_F for Galilean-invariant systems even in settings that are far removed from such a limit; in moiré systems with a nearly diverging m_{\star} at the single-particle level (i.e., for flat bands), interpreting the measurements in terms of such a T_F can be potentially problematic. Second, within standard BCS theory (and away from any dilute limit), we do not expect T_c to be limited by T_F in the observed fashion at all. Interestingly, in a Galilean invariant system, the zero-temperature superfluid stiffness of the superconductor is proportional to the bare T_F [24], and does not depend on the interaction strength. This raises the question of whether the observations by Uemura and coworkers are fundamentally controlled by a bound on T_c with respect to the zero-temperature stiffness. In light of these observations, a long-standing question is: Are there any universal upper bounds on superconducting T_c in generic correlated electronic solids that do not rely on a precise knowledge of the superconducting pairing mechanism?

3. A brief survey of IR-incomplete non-Fermi liquids

One of the cornerstones for describing conventional metals is Landau's Fermi liquid theory [25], developed originally for neutral He-3 atoms but which can be generalized to electrons in a straightforward fashion [26]. A remarkable outcome of Landau's original treatment, which was beautifully clarified using a more modern Wilsonian renormalization group perspective [27], is that the strongly interacting electrons at the UV scale in a metal are effectively described in terms of low-energy renormalized electronic "quasiparticle" excitations (i.e., carrying the same quantum numbers as the bare electron). The lifetime for these quasiparticles becomes progressively longer as one approaches the sharply defined Fermi surface in a Fermi liquid. Boltzmann had already developed a powerful method to describe the dynamics of a density of particles, f_p , with momentum p, in a classical dilute gas of molecules in response to time-dependent external forces [28] a few decades before Drude,

$$\frac{\partial f_{\mathbf{p}}}{\partial t} + \mathbf{F} \cdot \nabla_{\mathbf{p}} f_{\mathbf{p}} = \mathcal{C}[f]. \tag{3}$$

The right-hand-side of Eq. (3) describes collisions between the molecules, which Boltzmann assumed to be statistically independent in a sufficiently dilute gas. Remarkably, in a Landau Fermi liquid, as a result of the Pauli-blocking effect inside the filled Fermi sea the Boltzmann treatment is applicable, but now the f_p 's measure the distribution of electronic quasiparticles and the collision term on the R.H.S. of Eq. (3) is given by

$$C[f] \propto -\int_{p_{1,2,3}} \cdots [f_{p} f_{p_{1}} (1 - f_{p_{2}}) (1 - f_{p_{3}}) - f_{p_{2}} f_{p_{3}} (1 - f_{p}) (1 - f_{p_{1}})], \qquad (4)$$

where the additional (1 - f) factors ensure that the final states of collisions are not occupied [26].

Our focus in these lectures will be on strongly interacting metallic phases that display T-linear resistivity over an intermediate range of temperatures, i.e., for $T \gtrsim T^*$. When the temperature drops below T^* , there is a crossover to a metallic regime that does not exhibit any T-linear resistivity. Importantly, in the examples we discuss here, T^* can not be pushed to zero by tuning any parameter. * The examples we discuss are not stable "non-Fermi liquids" with a T-linear resistivity down to zero temperature, and thus are not described by a T=0 infrared (IR) fixed point with a finite number of relevant perturbations. We dub them as "IR-incomplete" phases of compressible quantum matter [21]. Next we discuss a few examples of such behavior arising in a variety of distinct settings.

3.1. Electron-phonon scattering in equipartition regime

We have already encountered a familiar example of an IR-incomplete metallic state that exhibits T-linear resistivity — the electron-phonon problem where T^* represents the characteristic Debye or Bloch-Grüneissen temperature [1, 15]. The origin of this behavior arises from the high-temperature behavior of the collision integral in Eq. (4), which depends on the phonon occupation number via the Bose-Einstein distribution, $n_B(T) \approx T/T^*$. Thus in effect, the phonons with their unbounded Hilbert space act as a source of quasi-elastic scattering at these high temperatures. Let us also note in passing that while one might question whether the Boltzmann prescription is valid in the above regime, where the single-particle self-energy $\text{Im}\Sigma(\omega,T) \sim \{\omega,T\}$, it was pointed out in the seminal work of Prange and Kadanoff [29] in the context of the same problem t hatapplying the Boltzmann equation does not rely on the existence of long-lived quasiparticles, provided that the self-energy is primarily frequency dependent with no (or rather weak) momentum dependence.

Why then is the ubiquitous T-linearity of resistivity across correlated systems not attributed to electron-phonon scattering (with some exceptions [30, 31])? It has been widely argued that the non-Fermi liquid parent states of high-temperature superconductors are not due to this mechanism [7, 8]. The arguments are based primarily on three points: (i) The T-linearity persists down to temperatures that are significantly lower than $T^* \approx Cv_sk_F$ for acoustic phonons with velocity v_s , or $T^* \approx C\omega_0$ for optical phonons with frequency ω_0 , where $C \lesssim 1$ is a numerical prefactor. (ii) Matthiessen's rule would suggest that coupling to multiple well-separated phonon branches would lead to T-dependent crossovers, which are typically not observed (at least in special regions of the phase diagrams; see Ref. [32] for a counterexample). (iii) Some of the most striking low-temperature T-linearity is often restricted to special points (suggestive of possible quantum critical points) or regions (suggestive of a quantum critical phase) especially in heavy-fermion based compounds [33], which

^{*}This is ignoring the obvious issue of superconducting instabilities that might interfere with the intrinsic normal state properties; we assume here that T_c can be suppressed via other means to reveal the metallic normal state.

highlights the importance of an electronic mechanism.

We will revisit the relevance of electron-phonon scattering and its more complex generalizations in Sec. 3.4 below in the context of some intriguing experiments on a real material. This will also lead us to speculate on potentially interesting scenarios that could provide a way around each of these concerns by invoking strong (and previously ignored) electron-phonon interactions that renormalize the phonon properties themselves. However, we will first discuss examples of T-linear resistivity in somewhat unconventional and correlated metallic liquids with very short-distance correlations in the next two sections.

3.2. Hot quantum matter in ultracold atom simulators

In this section, we will depart from the Landau-Boltzmann paradigm for describing transport associated with low-energy excitations near an electronic Fermi surface. Instead, we return to first-principles linear-response theory (i.e., the Kubo formula) and obtain the generic form of the current-current correlation function and the optical conductivity using the Lehmann representation [34],

$$\sigma(\omega, T) = \pi \frac{1 - e^{-\beta\hbar\omega}}{\omega Z} \sum_{n,m} e^{-\beta E_n} |J_{nm}|^2 \delta(E_n - E_m - \hbar\omega).$$
 (5)

Here, the eigenstates of the general many-body Hamiltonian are represented using indices n, m with energies E_n , E_m , respectively. The total current operator, J, has matrix elements J_{nm} between states n, m. Finally, $Z = \sum_n e^{-\beta E_n}$ denotes the partition function with $\beta^{-1} = T$. Note that the β -dependence enters only via the Boltzmann probabilities. One of the advantages of the above expression is that it can be applied, in principle, to any problem provided the many-body eigenspectrum is available; this includes problems with and without quasiparticles. Since the general framework for computing transport does not depend on the presence of an underlying Fermi surface, we will focus on interacting problems in regimes far from any renormalized Fermi-liquid-like description in the remainder of this (and next) section. The highly correlated metallic regimes we discuss will exhibit only short-ranged correlations in real space and no associated sharp structure in momentum space.

Consider the regime where T represents the largest energy scale in the problem for models with a bounded Hilbert space. In the dc limit ($\omega \to 0$), the leading contribution to a high-temperature (i.e., small β) expansion yields a deceptively simple expression for the conductivity:

$$\sigma(\omega, T) = \frac{\pi\hbar}{k_B T} \frac{1}{Z} \sum_{n,m} |J_{nm}|^2 \delta(E_n - E_m - \hbar\omega).$$
 (6)

For generic non-integrable lattice models where the sum remains finite in the thermodynamic limit, this immediately yields T-linear resistivity. The non-integrable nature is crucial as it produces "random-matrix-like" matrix elements J_{nm} even without explicit randomness [35]. The above program has been extended further on the

theoretical side to incorporate corrections that are higher-order in β [36, 37], and on the numerical side to evaluate the transport proxies using sophisticated numerical methods [38, 39, 40].

While Eq. (6) readily yields T-linear resistivity, examining this behavior through Einstein relations — which follow from local charge equilibration — proves instructive. Ignoring thermoelectric effects [41], the dc conductivity σ_{dc} , charge diffusion coefficient D_c , and charge compressibility χ_c are related via,

$$\sigma_{dc} = \chi_c D_c, \quad \chi_c = \frac{\partial n_c}{\partial \mu},$$
 (7)

where n_c represents the average density and μ is the chemical potential. In the high-temperature limit, when the electrons realize a "hot-soup", or a non-degenerate liquid, the $\sigma_c \sim 1/T$ behavior is controlled by the $\chi_c \sim 1/T$ piece, and a temperature independent D_c (or equivalently, scattering rate). Thus while this extremely high-temperature regime is far from resembling any degenerate electronic liquid with sharp spectral features in momentum-space, the T-linear resistivity is not tied to any Planckian scattering rate. However, this regime is characterized by "bad-metallic" conduction with $D_c \sim a^2/\tau_0$, where a is the lattice spacing and τ_0 is a timescale controlled by the microscopic energy scales (that vanish when $t \to 0$). It is as if the diffusion coefficient becomes bounded while the compressibility remains unbounded.

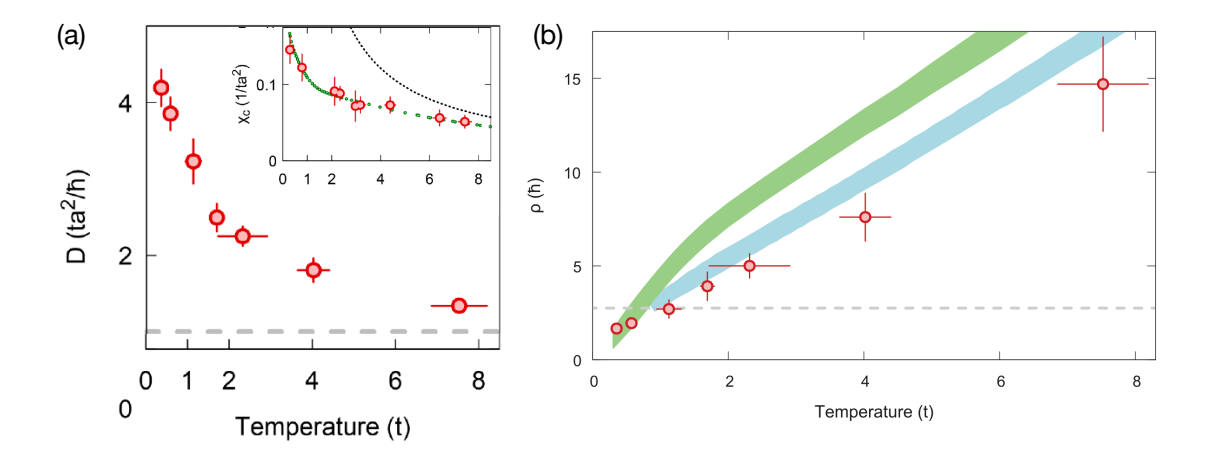


Figure 1. Temperature-dependent measurement of (a) charge diffusion and compressibility (inset) for a gas of ultra-cold ⁶Li atoms in a quantum microscope realizing a 2D Fermi-Hubbard model with $U/t \simeq 7.5$ at a density $n \simeq 0.825$. (b) Inferred resistivity using Einstein relation. Grey horizontal dashed lines represent point at which $k_F \ell \sim 1$. Theoretical calculations using DMFT (in green) and the finite-T Lanczos method (in blue) are shown. Adapted from Ref. [42].

In traditional solid-state systems, this bad-metallic T-linear resistivity regime lacks practical relevance, particularly given their numerous phonon branches and their unbounded spectra. However, ultracold atomic gases in optical lattices provide an

excellent experimental platform for analyzing this regime. A recent experiment [42] directly measured the diffusion constant and compressibility (Fig. 1a) to determine the resistivity for a spinful two-dimensional Hubbard model quantum simulator across a wide but relatively "hot" temperature window, $T/t \approx 0.3 - 8$. These measurements confirm that the high-temperature regime ($\chi_c \sim 1/T$, $D_c \sim \text{const}$) is indeed observed. Mysteriously, however, while both χ_c and D_c exhibit T-dependent crossovers with decreasing temperature, $\rho = [\sigma_c]^{-1}$ retains its T-linear behavior without noticeable crossovers or slope changes (Fig. 1b). Although the microscopic origin of this robust T-linear behavior remains unclear, it can be reformulated as follows. Returning to Eq. (5), one can formulate general conditions on the matrix element sum structure that preserve the T-linear resistivity slope [43]. This condition has been tested against numerical exact diagonalization results across various lattice models for small systemsizes. The fundamental question inspired by the cold-atom experiment is: What is the underlying principle that connects the smooth evolution from the "high" temperature regime (with a T-independent D_c) to the "low" temperature regime (with $D_c \sim 1/T$) without any noticeable change in the magnitude of $d\rho/dT$?

3.3. Charge frustrated bad metals

One might conclude that the aforementioned route to T-linear resistivity requires temperature to be the largest energy scale in the problem. However, this constraint is not necessary. As an explicit counterexample, we construct a "solvable" model at strong interactions exhibiting a broad regime of intermediate temperatures with T-linear resistivity driven by $\chi_c \sim 1/T$. Consider a model of interacting spinless fermions on the triangular lattice with a Hamiltonian,

$$H = H_t + H_V, (8a)$$

$$H_t = -t \sum_{\langle \boldsymbol{r}, \boldsymbol{r}' \rangle} \left(c_{\boldsymbol{r}}^{\dagger} c_{\boldsymbol{r}'} + \text{H.c.} \right) - \mu_c \sum_{\boldsymbol{r}} n_{\boldsymbol{r}}^c, \tag{8b}$$

$$H_V = V \sum_{\langle \boldsymbol{r}, \boldsymbol{r}' \rangle} \left(n_{\boldsymbol{r}}^c - \frac{1}{2} \right) \left(n_{\boldsymbol{r}'}^c - \frac{1}{2} \right), \tag{8c}$$

where t is a nearest-neighbor hopping and V is a nearest-neighbor repulsive interaction strength, respectively. The fermion density at \mathbf{r} is, $n_{\mathbf{r}}^c = c_{\mathbf{r}}^\dagger c_{\mathbf{r}}$ (= 0, 1), and the global density can be tuned via the chemical potential, μ_c . It is worth pointing out that the local Hilbert space dimension is 2 and the interaction-only limit (t = 0) is described by the frustrated antiferromagnetic Ising model on the triangular lattice, for which a number of exact results are known [44, 45, 46, 47], which will be useful when we solve the model at strong-coupling.

At asymptotically weak coupling, $\lambda(=V/t) \ll 1$, the ground state constitutes a Fermi liquid with a sharply defined Fermi surface, and transport can be analyzed using conventional Boltzmann equation approaches for low-energy Landau quasiparticles. In the clean limit, Umklapp scattering degrades momentum, and for densities where the

Fermi surface is sufficiently large (i.e., occupies a significant portion of the Brillouin zone), we expect $\rho_{\rm dc} \sim (h/e^2) \overline{V}^2 (T/T_F)^2$, where \overline{V} represents a dimensionless interaction strength and T_F denotes the Fermi temperature. The resulting state is a "good" metal with $\rho_{\rm dc} \ll h/e^2$. In contrast, at strong coupling $\lambda \gg 1$, the ground-state properties of this Hamiltonian remain unknown; the model suffers from the infamous "sign- problem" and is not amenable to quantum Monte Carlo methods. Nevertheless, inspired by numerically exact studies of a hardcore boson version of the same model on the triangular lattice [48, 49, 50], we can speculate that the ground state is likely (i) a renormalized Fermi liquid over a wide range of λ , particularly away from commensurate fillings, and (ii) exhibits additional charge density-wave correlations over a range of commensurate fillings near 1/3 < n < 2/3.

We address the following question next: Consider the intermediate to high temperature regime (i.e., temperatures exceeding any "coherence" scale associated with a renormalized Fermi liquid). Let us analyze the problem perturbatively from the strong-coupling limit (t=0). Since the electron current operator scales as O(t), we observe that $\sigma(\omega, T) \propto t^2$ in Eq. (5). However, in this perturbative limit, thermal expectation values can be evaluated within the purely classical theory at t=0. Thus, the T and V dependence of $\sigma(\omega, T)$ arises solely from the short-ranged correlators of the density operators on nearest-neighbor sites connected by electron hops. The conductivity at a finite frequency, ω is then given by [51, 52], *

$$\sigma(\omega) = \frac{e^2}{h} t^2 \frac{1 - e^{-\beta\hbar\omega}}{\hbar\omega} \sum_{\{n\}} \frac{e^{-\beta H_{t=0}(\{n\})}}{Z} \frac{2\pi^2}{\text{vol}} \sum_{\langle \boldsymbol{r}, \boldsymbol{r}' \rangle} (D_{\boldsymbol{r}\boldsymbol{r}'}^x)^2 \Delta_{\boldsymbol{r}\boldsymbol{r}'}(\omega), \tag{9}$$

where $D_{rr'}^x$ is the x component of the vector $D_{rr'} = r - r'$ for the longitudinal response in the x-direction, and

$$\Delta_{rr'}(\omega) = n_{r'}(1 - n_r) \, \delta(\hbar\omega - \varepsilon_r^f + \varepsilon_{r'}^i). \tag{10}$$

Eq. (10) has an intuitive explanation: the $n_{r'}(1-n_r)$ piece takes into account the probability for an electron to hop between the two nearest-neighbor sites \boldsymbol{r} and \boldsymbol{r}' depending on their occupancies, and enumerates the number of excitations with energy $\hbar\omega$ that can be generated via the hop. The energy difference corresponds to moving an electron at \boldsymbol{r}' with local energy $\varepsilon_{\boldsymbol{r}'}^i$ to a nearest neighbor site \boldsymbol{r} with local energy $\varepsilon_{\boldsymbol{r}'}^f$. Relatedly, the expectation value in Eqn. 9 effectively amounts to computing the histogram of $\Delta\varepsilon_{\boldsymbol{r}\boldsymbol{r}'} = \varepsilon_{\boldsymbol{r}'}^f - \varepsilon_{\boldsymbol{r}'}^i$.

Before examining the results for σ , we discuss the charge compressibility χ_c . Across a broad range of fillings, χ_c exhibits characteristic $\chi_c \sim 1/T$ dependence at both high $(T \gg V)$ and low temperatures $(T \ll V)$, albeit with different prefactors. The high-T limit parallels the results from the previous section. Additionally, in the t=0

^{*}The t=0 limit has a massive degeneracy and requires degenerate perturbation theory for a small t. Instead, the degeneracy can be lifted by including e.g. a weaker longer-ranged screened Coulomb interaction without affecting the transport properties in a qualitative fashion at the temperatures of interest.

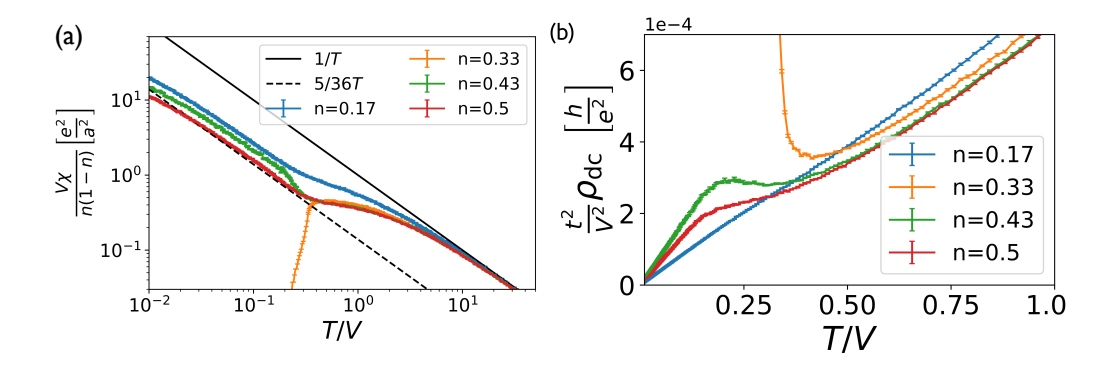


Figure 2. Temperature-dependence of: (a) compressibility obtained from Monte-Carlo computations showing distinct regimes of a 1/T scaling connected by a smooth crossover. The solid and dashed lines correspond to asymptotic expansions for χ at high and low temperatures, respectively. (b) dc resistivity for a few representative fillings. Adapted from Ref. [51].

limit, the system maps onto the frustrated Ising spin model on the triangular lattice, where the magnetic susceptibility in the spin representation directly corresponds to the charge compressibility in the electronic description. Remarkably, at half-filling, this correspondence yields an exact result for χ_c [53, 54]. The numerical simulations reproduce this analytic result (see Fig. 2a), revealing a smooth crossover between the high- and low-temperature 1/T behavior at the characteristic scale $T \sim V$. Similar qualitative trends emerge at other non-commensurate fillings, though with varying slopes in the low-temperature regime. At commensurate fillings (e.g., n = 1/3), the system undergoes a transition into an ordered phase with a precipitous drop in χ_c , as expected in the strong-coupling limit.

Direct computation of the resistivity based on Eq. (9) in the $\omega \to 0$ limit (see Fig. 2b) reveals several interesting aspects. At commensurate filling (n=1/3), the high-T metallic regime directly crosses over into the insulating crystal. For other generic fillings, a smooth crossover occurs between two distinct regimes of T-linear resistivity, both largely dominated by the T-dependent χ_c . However, given the relatively smooth thermodynamic evolution as a function of filling, there exists a narrow range of fillings (see e.g., data at n=0.17) where, despite the relatively distinct behaviors of χ_c at high and low T, the resistivity appears to exhibit no clear change in its T-dependence over a wide temperature range. See Ref. [51] for more detailed discussion of the additional structure in the data.

We conclude by noting that both the high to intermediate-temperature mechanisms for T-linear and "bad" metallic resistivity are distinct from "Planckian" scattering-dominated transport at low temperatures, that is ubiquitous across solid-state systems. In the former, charge diffusivity saturates with increasing temperature and is bounded by short-distance physics, while in the latter a sharp bound on the scattering rate (if it exists) is presently unavailable. It is widely believed that the scattering rate in the

correlated materials of interest is T-linear rather than the compressibility; a recent interesting exception has been observed in CeCoIn [6]. Establishing this distinction is generally difficult without optical measurements. Remarkably, recent advances have enabled direct measurements of electronic compressibility in two-dimensional gate-tunable materials in the Planckian regime of MATBG [55]. Finally, we note that the above models should not suggest that Planckian scattering rates are mutually exclusive with bad metallicity (and short-ranged correlations), since there exist explicit models (e.g., lattice constructions of Sachdev-Ye-Kitaev dots [56, 57, 21]) where the two phenomena coexist. Given the difficulties in describing non-trivial regimes of Planckian transport in real materials starting from first-principles, we turn to an interesting example in the next section where such an attempt has been made successfully.

3.4. Bottom-up approach: Planckian transport in magnetic delafossites

As noted previously, electrons scatter off impurities, other electrons, lattice vibrations, and collective excitations when propagating through even the cleanest quantum Isolating the contribution from electron-electron interactions while materials. maintaining detailed microscopic understanding of the electronic structure remains challenging. This motivates studying materials that enable controlled investigation of different scattering mechanisms. The delafossite compounds [58], PdCoO₂ and PdCrO₂ provide an ideal controlled experiment, as they share an identical crystal structure (Fig. 3a) — alternating layers of highly conducting Pd sheets and insulating oxide layers (CoO₂ or CrO₂) arranged in triangular lattices — but exhibit dramatically different transport properties. In PdCoO₂, the CoO₂ layers form a conventional band insulator with an O(eV) charge gap and no low-energy magnetic excitations. Conversely, in $PdCrO_2$, the CrO_2 layers form a Mott insulator with localized S = 3/2 magnetic moments that undergo antiferromagnetic ordering below $T_N \approx 37.5$ K, highlighting its strongly correlated nature. This material pair enables nearly perfect experimental control: they possess virtually identical phonon spectra due to their shared structural motif, * while their electronic spectra differ drastically. Both materials also exhibit exceptional metallic conductivity with long mean-free paths $(k_F \ell \gg 1)$, confirming their relatively clean nature.

Despite their structural similarities, transport measurements reveal striking differences between these compounds [59]. While both are highly conducting metals, PdCrO₂ exhibits significantly higher resistivity than PdCoO₂ across a wide temperature range. Most remarkably, PdCrO₂ displays pronounced T-linear resistivity extending from approximately O(100) K up to the highest measured temperatures. The excess resistivity $\Delta = \rho(T) \begin{vmatrix} & -\rho(T) \\ & \text{PdCrO}_2 \end{vmatrix}$ grows linearly with temperature in this regime (Fig. 3b), and Drude analysis reveals the transport scattering rate has Planckian form [61]. Empirically, PdCrO₂ appears to provide an example of an IR-incomplete

^{*}Except for the differences that arise from the weights of Co vs. Cr.

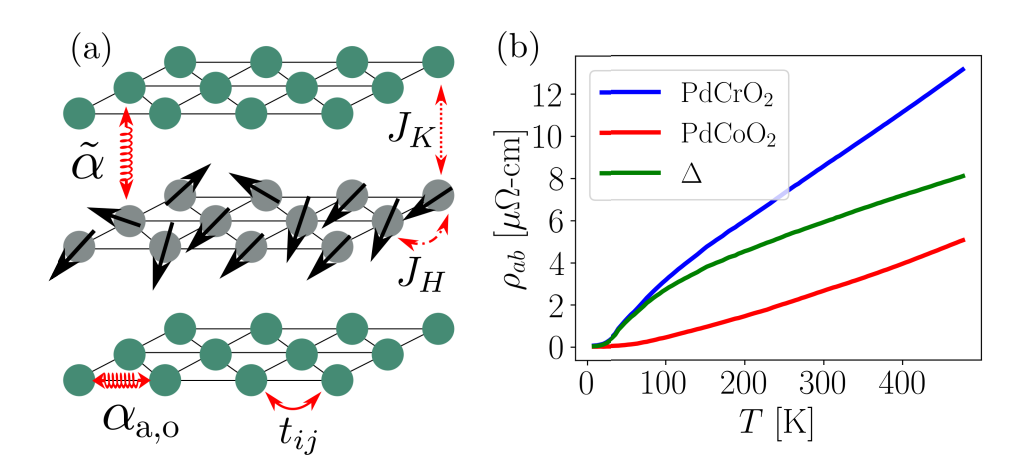


Figure 3. (a) Structure of PdCrO₂, consisting of alternating layers of triangular lattices of conducting Pd planes (green) and Mott insulating CrO₂ planes (grey). The coupling constants denoted in the figure are introduced in Eq. (11a) and Eq. (12c). (b) The inplane resistivities of PdCrO₂ and PdCoO₂ taken from Ref. [59] along with their difference $\Delta \rho \equiv \rho_{ab}^{\rm PdCrO_2} - \rho_{ab}^{\rm PdCoO_2} > 0$. Adapted from Ref. [60]

metallic phase where T-linear resistivity does not extend to the lowest temperatures. Controlled electron-irradiation experiments on PdCrO₂ reveal that increased dosage only increases the residual resistivity $\rho(T \to 0)$, reflecting enhanced elastic scattering from impurities, while the T-linear resistivity slope remains unchanged [61]. This highlights the intrinsic origin of Planckian transport and demonstrates a Matthiessen-like behavior in the transport scattering rates. This behavior mirrors similar experiments in electron-irradiated cuprates [62], where T-linear resistivity slope remains unchanged with dosage while superconducting T_c and residual resistivity are affected as expected. Moreover, the observations pose a fundamental question: given essentially identical phonon spectra between the two compounds, such that traditional electron-phonon interactions cannot account for this difference, what causes the enhanced T-linear resistivity in PdCrO₂?

The microscopic degrees of freedom and their couplings are well characterized through spectroscopic measurements in both compounds [63]. To understand electrical transport in these layered metal/Mott-insulator systems, we construct a minimal theoretical model capturing all relevant interactions and momentum-relaxation scattering processes. The electronic dispersion, dominated by Pd electrons, has been directly measured by ARPES in both compounds [64]. The Fermi surface is approximately circular with area roughly half the Brillouin zone, readily modeled by standard tight-binding with dispersion ε_k and chemical potential μ . The magnetic subsystem consists of localized Cr moments interacting via predominantly nearest-neighbor antiferromagnetic Heisenberg exchange J_H . These interactions determine the ordered state below T_N , but local moments exhibit significant dynamic fluctuations above T_N that scatter conduction electrons. The coupling between conduction electrons

and local moments has been directly extracted through spectroscopic measurements, revealing antiferromagnetic Kondo exchange J_K (Fig. 3a). To summarize, the low-energy Hamiltonian is given by,

$$H = H_{\rm el} + H_{\rm S} + H_{\rm K},$$
 (11a)

$$H_{\rm el} = \sum_{\mathbf{k}\alpha} (\varepsilon_{\mathbf{k}} - \mu) p_{\mathbf{k}\alpha}^{\dagger} p_{\mathbf{k}\alpha}, \tag{11b}$$

$$H_{\rm S} = J_{\rm H} \sum_{\langle i,j \rangle} \boldsymbol{S}_i \cdot \boldsymbol{S}_j, \quad H_{\rm K} = J_{\rm K} \sum_i p_{i\alpha}^{\dagger} (\boldsymbol{S}_i \cdot \boldsymbol{\sigma}_{\alpha\beta}) p_{i\beta},$$
 (11c)

The Kondo scattering mechanism alone cannot produce T-linear resistivity. Previous theoretical work shows that electrons scattering off fluctuating local moments in the paramagnetic phase produce a scattering rate that grows sublinearly with temperature before saturating to a temperature-independent value for $T \gg J_H$ [65]. This behavior reflects that magnetic correlations are bounded and become increasingly short-ranged as temperature increases, unlike high-temperature phonons that occupy an unbounded Hilbert space where occupation increases as $n_B(T)$.

The crucial insight for resolving this puzzle involves recognizing a previously ignored interaction term: an electron-magneto-elastic (EME) coupling [60]. Consider the modified Hamiltonian starting from Eq. (11a), $H \rightarrow (H + H_{\rm ph} + H_{\rm el-ph} + H_{\rm EME})$, where (Fig. 3a)

$$H_{\rm ph} = \sum_{\ell=I_{\rm a},I_{\rm o},O} \sum_{\mathbf{q}} \left(\frac{|\pi_{\mathbf{q}}^{(\ell)}|^2}{2M} + \frac{M\omega_{\ell,\mathbf{q}}^2}{2} |\varphi_{\mathbf{q}}^{(\ell)}|^2 \right), \tag{12a}$$

$$H_{\rm el-ph} = \sum_{i,\sigma} \left(\alpha_{\rm a} \nabla \varphi_i^{(I_{\rm a})} p_{i\sigma}^{\dagger} p_{i\sigma} + \alpha_{\rm o} \varphi_i^{(I_{\rm o})} p_{i\sigma}^{\dagger} p_{i\sigma} \right), \tag{12b}$$

$$H_{\rm EME} = \widetilde{\alpha} \sum_{i} \varphi_{i}^{(O)} p_{i\alpha}^{\dagger} (\boldsymbol{S}_{i} \cdot \boldsymbol{\sigma}_{\alpha\beta}) p_{i\beta}. \tag{12c}$$

Physically, this coupling arises because the interlayer distance directly affects the hybridization between Pd and Cr electronic states, i.e. of the form $p_{i\sigma}^{\dagger}c_{j\sigma}(1-\alpha X_{ij})$, which in turn controls the effective Kondo coupling strength. When the lattice vibrates in the out-of-plane direction, it periodically strengthens and weakens this magnetic interaction, creating a new channel for electron scattering that combines phononic and magnetic degrees of freedom. Note that when $J_H = J_K = \tilde{\alpha} = 0$, the above model essentially describes the theory for PdCoO₂ (except for the slight differences in the values of ω_{ℓ}). Given the long mean-free paths and a relatively detailed understanding of the (weak) couplings between the distinct degrees of freedom, apart from the EME coupling, we can employ the Landau-Boltzmann framework to calculate the total scattering rate according to Matthiessen's rule. In PdCoO₂, this would be $1/\tau_{\rm tr} = 1/\tau_{\rm el-ph}$, while in PdCrO₂, due to the additional sources of scattering this amounts to, $1/\tau_{\rm tr} = 1/\tau_{\rm el-ph} + 1/\tau_{K} + 1/\tau_{\rm EME}$.

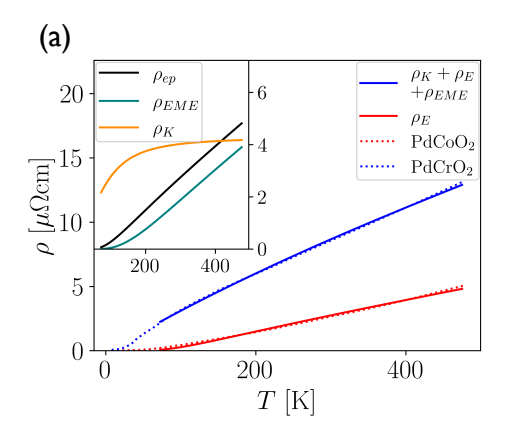
Let us first consider the scattering rate in the asymptotic limit of high-temperatures. The conventional acoustic electron-phonon scattering produces the familiar, $1/\tau_{\rm el-ph,a} \propto$

 $\lambda_{\rm el-ph,a}T$, where the dimensionless coupling constant $\lambda_{\rm el-ph,a} = \nu_0 \alpha_a^2/(Mc^2)$ depends on the density of states ν_0 , the electron-phonon coupling α_a , the ionic mass M, and the sound velocity c. The optical phonons contribute a more complex temperature dependence, $1/\tau_{\rm el-ph,o}$, depending on the ratio ω_0/T , starting from an exponentially suppressed behavior at asymptotically low temperatures to the standard T-linear behavior at high temperatures. As noted above, the Kondo scattering off the fluctuating Cr-local moments leads to a saturation of the rate at high temperatures. Finally, let us turn to the EME scattering mechanism. Unlike conventional electron-phonon or electron-magnetic scattering, the EME process involves a three-body interaction where an electron simultaneously scatters off independent magnetic moments and out-of-plane phonons. However, at the relatively high temperatures of interest, the former does not contribute any temperature dependence while the latter provides the usual quasi-elastic T-linear scattering rate. This leads to a scattering rate, $1/\tau_{\rm EME} \propto \lambda_{\rm EME} T$, where the effective coupling strength is $\lambda_{\rm EME} = \nu_0 \tilde{\alpha}^2 S(S+1)/(M\tilde{\omega}_0^2)$. Thus the enhancement in the slope of the T-linear resistivity in PdCrO₂ is directly affected by the total scattering cross-section provided by the Cr-local-moments.

The EME interaction mechanism exhibits several distinctive features that enhance its effectiveness. First, the out-of-plane phonon frequency $\tilde{\omega}_0$ is naturally softer than in-plane modes due to weaker interlayer bonding, increasing the scattering cross-section. The magnetic enhancement factor S(S+1)=15/4 for S=3/2 Cr moments significantly amplifies the scattering rate coefficient even when the bare dimensionless coupling is weak. Most importantly, unlike conventional electron-phonon scattering constrained by small-angle processes, EME enables large momentum transfer because interacting local moments with short correlation length can absorb momentum, effectively functioning as a bath. Finally, experimental support for this proposal comes from the observation of Wiedemann-Franz law $\kappa/\sigma T \sim L/L_0 \rightarrow 1$ in the T-linear resistivity regime, confirming a quasielastic scattering source consistent with the EME mechanism [61].

A striking observation emerges from a detailed Boltzmann computation of scattering rates using the known couplings and our conjectured EME coupling (treated as a fit parameter). As shown in Fig. 4(b), neither electron-phonon, Kondo, nor EME contributions are individually linear — each exhibits a non-trivial T—dependence. Nevertheless, their sum produces a Planckian form with an O(1) coefficient. The deeper question of why these scattering rates sum to a Planckian form remains an open question. Is this a coincidence or does it reflect some underlying fundamental bound? A recent idea inspired by a study of the Holstein model suggests a "stability-bound" on the dimensionless coupling constant [66], before the metallic state becomes unstable to competing orders. However, in the above system this putative bound appears to apply to a total scattering rate, not just the electron-phonon contributions. The generalization of such a bound to coupling constants that induce an inelastic scattering rate is presently unknown.

As we conclude this section, it is worth asking whether this material provides insights into similar mechanisms for T-linear resistivity in other systems. The above



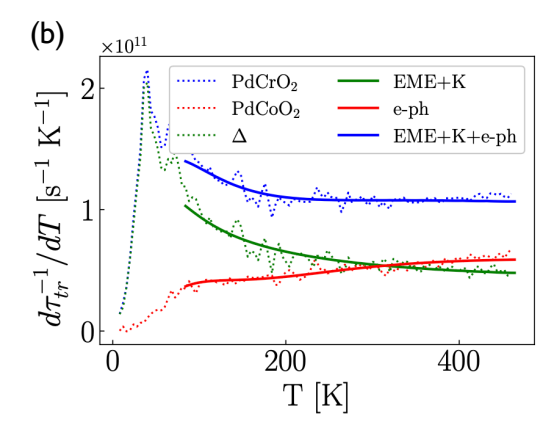


Figure 4. (a) Comparison of in-plane resistivity between experiments [59] (dotted lines) and the model in Eq. (11a) and (12c) (solid lines). The free fit-parameters are the out-of-plane phonon frequency and bare el-ph and EME couplings. All other parameters are fixed; see Ref. [64]. For the phonon data, we have used $\omega_D = 29 \text{meV}$, $\omega_0 = 120 \text{meV}$, $\widetilde{\omega}_0 = 40 \text{meV}$, $\lambda_{\text{el-ph,a}} = 0.04$, $\lambda_{\text{el-ph,o}} = 0.02$, $\lambda_{\text{EME}} = 0.05$ and S = 3/2. (b) Rate of change of scattering rate from fit (obtained from Boltzmann theory) and experiments. Adapted from Ref. [60].

mechanism demonstrates that phonons can intertwine with correlated electronic degrees of freedom to produce unexpected behavior. Notably, specific heat measurements show that local moments cause relative phonon softening (and reduced Debye temperature) in $PdCrO_2$ compared to the non-magnetic $PdCoO_2$ [61]. Returning to the key criticism that phonons cannot produce T-linear resistivity in strange metals, consider the following possibilities: while the bare phonon energy scales are presumably too high for low-T linearity, coupling to electronic degrees of freedom could induce a non-trivial softening. Simultaneously, the electron-phonon coupling could be enhanced up to some putative stability bound producing Planckian scattering rates. Finally, couplings to different phonon branches need not have equal strength, getting around Mathiessen's rule. Investigating these questions in concrete, solvable settings remains an exciting frontier.

4. Superconductivity is not boundless

All superconductors, regardless of their microscopic mechanism or pairing symmetry, exhibit two fundamental properties: zero electrical resistance and diamagnetism. These properties are intrinsically linked. Consider the universal form of their longitudinal optical response,

$$Re[\sigma(\omega)] = \frac{e^2}{h} D_s \ \delta(\omega) +, \tag{13}$$

where the coefficient of the δ -function response at zero frequency, D_s , is referred to as the superfluid stiffness. The symbols '...' denote corrections that depend on the low-energy spectrum in the superconductor, which is determined by factors such as

the energy gap (or its absence in nodal systems or due to disorder-induced bound states), collective modes, and other phenomena. Here we focus primarily on (quasi) two-dimensional superconductors, a category encompassing many intriguing and poorly understood systems including cuprates and moiré materials. The dominant contribution to the long-wavelength fluctuations in two-dimensional superconductors is governed by a free energy, F, associated with a complex order-parameter $\Psi = |\Psi_0|e^{i\theta}$, where,

$$F = D_s \int d^2 \mathbf{r} (\nabla \theta - 2e\mathbf{A})^2 + \dots$$
 (14)

Here e is the electron charge and A is the external vector potential that couples minimally to the charge—2e Cooper-pair represented by Ψ . The symbols '...' include higher order contributions to the free energy from the fluctuations of the order parameter. In general, $D_s(T)$ exhibits a non-trivial temperature dependence that inherently measures the strength of phase-fluctuations, and can be a sensitive probe of the interplay of the density of states associated with the low-energy Boguliobov excitations and disorder. In two-dimensional systems, D_s has dimensions of energy, and the superconducting transition follows the Berezinskii-Kosterlitz-Thouless universality class, where $T_c = 2D_s(T_c^-)/\pi$ [67]. Any universal understanding of T_c in (quasi) two-dimensional systems must therefore focus on the microscopic ingredients that limit D_s , making this a question of fundamental importance and far-reaching significance.

The above discussion reveals a crucial distinction between the energy scales limiting T_c . While D_s governs phase-ordering, there exists (generically) an independent energy scale associated with amplitude-ordering. Consider a two-dimensional Galilean invariant electron system with parabolic dispersion (with mass m and density n). The zerotemperature superfluid stiffness $D_s(T=0) = 4ne^2/m$ relates to the Fermi temperature — a large energy scale independent of the pairing gap and interaction strength. Conversely, the amplitude ordering scale in the weak-coupling BCS limit starting from a Fermi liquid normal state determines $T_c \sim \omega_0 e^{-1/g} (\lesssim \omega_0)$, where ω_0 is a characteristic energy scale (e.g., phonon mode) with dimensionless attraction strength $g \ll 1$. An uncontrolled extrapolation to $g \to \infty$ might suggest that T_c is limited by ω_0 , the only relevant energy scale that provides the attraction. However, beyond the weakly interacting limit in the absence of an a priori obvious Cooper instability of a Fermi liquid and potentially competing orders, one must reconsider which energy scale controls T_c . As we will see in the next section, optimizing one energy scale (e.g., pairing) to enhance T_c often degrades the other (e.g., phase-coherence) scale, fundamentally limiting achievable values of T_c .

4.1. Raising T_c — an optimization problem

We illustrate the competing tendencies of amplitude versus phase-ordering in a superconductor with increasing interaction strength using the attractive—U Hubbard

model with nearest-neighbor hopping on the square lattice,

$$H = \sum_{\langle i,j\rangle,\sigma} (-t - \mu \delta_{ij}) c_{i,\sigma}^{\dagger} c_{j,\sigma} - \frac{|U|}{2} \sum_{i} n_{i} (n_{i} - 1), \tag{15}$$

where $n_i = \sum_{\sigma} c_{i,\sigma}^{\dagger} c_{i,\sigma}$ and μ is the chemical potential. The dimensionless interaction strength can be considered to be g = |U|/t. For $g \ll 1$, we expect a mean-field like transition to superconductivity with $T_c^{\text{MFT}} \sim |U|e^{-\alpha t/|U|}$, where α is an O(1) number. To go beyond the weak-coupling limimt, where perturbation theory in |U|/t is likely to fail and the fate of the metallic state above a putative superconducting T_c is a priori unclear, one can employ the numerically exact quantum Monte-Carlo (QMC) method [68]. The absence of the infamous "sign-problem" is due to time-reversal symmetry at any band filling and enables an exact solution. With increasing |U|/t, T_c reaches a maximum value around $t \sim |U|$, and then decreases (Fig. 5a). Interestingly, the spingap scale from spin susceptibility increases monotonically [69], indicating pair-formation at high temperatures without any onset of superconductivity at the same scale. This implies that while pair-formation leads to a finite local expectation value for $|\Psi_0|$, longrange phase-coherence is absent. In order to understand the suppressed T_c , one can start from the strong-coupling limit (i.e., t=0) where the ground state is a massively degenerate liquid of fully localized Cooper-pairs. Turning on a finite t reveals a finite energy scale associated with the hopping of Cooper-pairs, $t^2/|U|$, which is precisely the D_s scale (phase-stiffness relates directly to Cooper-pair kinetic energy). Thus in the strong-coupling limit, T_c is no longer limited by the gap-size, |U|, but by D_s . Moreover, the transition is highly non-BCS-like since the normal state above T_c is not a Fermi liquid with a sharp Fermi surface, but a phase-incoherent liquid of gapped Cooper pairs.

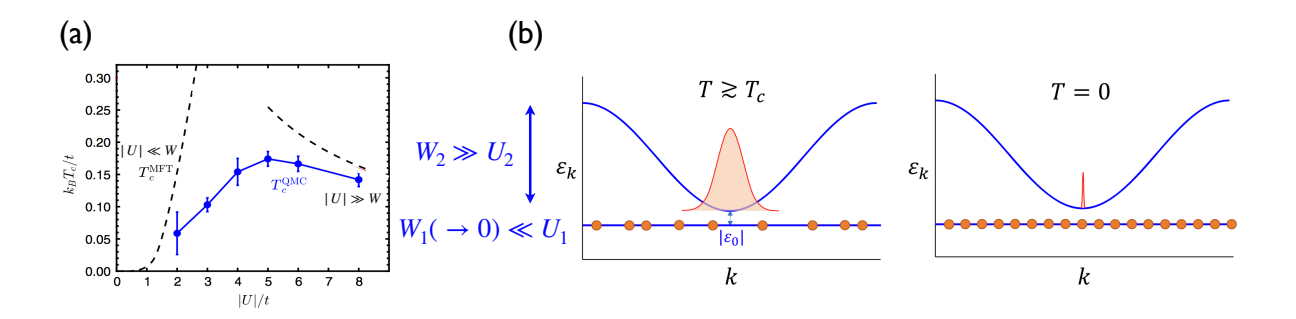


Figure 5. (a) Numerically exact solution for T_c obtained using QMC (blue) for the model in Eq. (15), along with the BCS prediction for T_c^{MFT} at weak-coupling and $t^2/|U|$ at strong-coupling. Adapted from Ref. [69] (b) Schematic illustration of the model in Eq. (16a), along with the dispersions and momentum distribution functions for the bosons. Adapted from Ref. [70].

This analysis illustrates a fundamental principle underlying the challenge of increasing T_c in models with two separate energy scales (e.g., t and |U|): enhancing the pairing scale by increasing attraction strength comes at the cost of degrading the

phase-stiffness. This raises two important questions: (i) What sets T_c in the limit of a vanishing bandwidth, as in "flat" bands central to tunable moiré materials, when interactions provide the only energy scale? (ii) Does D_s serve as a fundamental upper bound on T_c ?

Let us briefly address both questions before elaborating in the next two sections. In the limit $t \to 0$, $D_s \to 0$ in the above example. However, this limit is pathological as the lattice becomes disconnected, making the resulting classical model non-superconducting. Conversely, flat bands relevant to isolated bands in moiré materials arise from subtle quantum mechanical interference effects. The (de-)localization properties of any Wannier function constructed for the flat band are determined by their Bloch wavefunctions (quantum geometry) [71]. In the extreme limit of a completely quenched kinetic energy, interactions provide the only relevant low-energy scale. If the ground state is superconducting, T_c and D_s must be set by the interaction scale [72]. Explicit "solvable" examples show that one of the ingredients determining T_c (and D_s) is the integrated Fubini-Study metric [73, 74, 75, 76, 77]; however, a non-zero metric with attractive interactions does not guarantee superconducting ground states as competing orders can arise generically [73, 77]. For superconducting states that arise in models with topologically trivial flat bands, $T_c/|\Psi_0| \rightarrow 0$ can be realized in an "atomic" Fundamentally, no lower bound exists on superconducting T_c under generic circumstances. This raises the question of what sets possibly tight upper bounds on T_c , both in generic electronic models and in low-energy models relevant for moiré superconductivity.

4.2. Revisiting upper bounds on $T_c/D_s(0)$

The empirical observation of a seeming bound on T_c in terms of a "proxy" for E_F [22] suggests that the zero-temperature superfluid stiffness $D_s(0)$ plausibly serves as a fundamental upper bound on superconducting T_c [78]. This reasoning stems from the BKT relation $T_c = \pi D_s(T_c)/2$, combined with the assumption that $D_s(T)$ decreases monotonically with temperature, yielding $D_s(0) \geq D_s(T_c)$. The zero-temperature phase stiffness can be extracted experimentally from London penetration depth $\lambda_L^2(0) \propto 1/D_s(0)$ or low-frequency optical conductivity measurements [79]. While this reasoning applies to many stiffness-limited superconductors, no fundamental bound exists on $T_c/D_s(0)$ [70]. The physical inspiration for violating such bounds connects, e.g. to experimental observations in Zn-doped cuprates [80], highlighting fundamental limitations of phase-stiffness-based bounds on superconductivity.

As an explicit example, consider a two-dimensional lattice model with two species of complex bosons b_{α} ($\alpha = 1, 2$), with a Hamiltonian [70]

$$H = H_0 + H_{\text{int}}, \tag{16a}$$

$$H_0 = \sum_{\alpha, \mathbf{k}} \varepsilon_{\alpha}(\mathbf{k}) \ b_{\alpha, \mathbf{k}}^{\dagger} b_{\alpha, \mathbf{k}}, \quad H_{\text{int}} = \sum_{\alpha} \frac{U_{\alpha}}{2} n_{\alpha, \mathbf{r}} (n_{\alpha, \mathbf{r}} - 1). \tag{16b}$$

Let us assume that $\varepsilon_2(\mathbf{k})$ has a large bandwidth W_2 , and $\varepsilon_1 = \varepsilon_2(0) - \varepsilon_0$ forms a

completely flat and trivial band at energy ε_0 below the bottom of the ε_2 band (see Fig. 5b). We have included an on-site Hubbard interaction of strength U_{α} for the b_{α} bosons. The interaction term $H_{\rm int}$ includes an on-site Hubbard interaction with strengths $U_{1,2}$ for the $b_{1,2}$ bosons. Consider the limit $U_2 \ll W_2$ and $U_1 \to \infty$, imposing a hard-core constraint on the b_1 -bosons. Consider the total boson filling per unit cell to be $n_b > 1$. For the remainder of our discussion, we can simplify the problem by approximating $\varepsilon_2(\mathbf{k}) \approx \mathbf{k}^2/(2m_b)$ near the bottom of the broad band.

At temperatures near T_c , the chemical potential lies slightly above the bottom of the broad band. Assuming $T \gg \varepsilon_0$, the average occupation associated with the b_1 bosons on the localized sites approaches 1/2, since they behave as hard-core bosons at effectively infinite temperature. The remaining $(n_b - 1/2)$ bosons per unit cell occupy the broad band, leading to (upto additional logarithmic corrections) [81, 82, 83],

$$T_c \sim \frac{n_b - 1/2}{2m_b}.$$
 (17)

On the other hand, at T = 0 the localized sites associated with the b_1 bosons are fully filled with one boson. The density of bosons in the broad band now becomes $(n_b - 1)$, such that

$$D_s(0) \sim \frac{n_b - 1}{2m_b}.$$
 (18)

From Eqs. (17) and (18), the ratio becomes:

$$\frac{T_c}{D_s(0)} = \frac{n_b - 1/2}{n_b - 1}. (19)$$

Thus we immediately note that this ratio can be made arbitrarily large as $n_b \to 1^+$. In fact, when $1/2 < n_b < 1$, the ground state is not a superconductor (i.e. $D_s(0) = 0$), while $T_c > 0$; the physics involves "reentrant" superconductivity where the system becomes superconducting upon heating. The physical mechanism underlying this violation is that at high temperatures, the flat band is only half-filled on average, leaving more particles available for the dispersive band and enhancing T_c . At low temperatures, complete filling of the flat band depletes the dispersive band, suppressing $D_s(0)$. Thus, as a matter of principle, we can not have a fundamental upper bound on $T_c/D_s(0)$.

4.3. Fundamental upper bounds from optical sum-rules

To address which energy scales fundamentally bound T_c , we examine the origin of the spectral weight contained in the $D_s\delta(\omega)$ piece. Across a superconducting transition, a large fraction of the spectral weight contained in $\omega \in [0, 2\Delta]$ (where Δ is the largest SC gap-scale) is transferred to $\delta(\omega)$. However, as is well-known, the total optical spectral-weight is constrained and determined by only a few microscopic properties of the many-body Hamiltonian [85, 86], as we will now demonstrate by revisiting Eqs. (5) and (13).

^{*}In a similar vein, any putative upper bound on T_c/E_F (with an appropriately defined E_F) can also be violated by an arbitrary amount in explicit examples [70], highlighting that no such fundamental bound exists outside of the Galilean-invariant limit [84].

Thus, we can use optical sum-rules to constrain $D_s(0)$ [84]. Recall that the current operator $J_x = -ie[X, H]$, where the many-body position operator, $X = \sum_i x_i c_i^{\dagger} c_i$. Then, the expression for the integrated longitudinal conductivity starting from Eq. (5) becomes,

$$S = \int_0^\infty d\omega \operatorname{Re}[\sigma(\omega)] = -\frac{\pi}{2} \operatorname{Tr}\left(\hat{\rho}[X, [X, H]]\right), \tag{20a}$$

where $\hat{\rho}$ is a density matrix associated with either a thermal state, or ground-state projector. Focusing on T = 0, we can bound $D_s(0) \leq \mathbb{S}$.

As a first simple application of this sum-rule, consider a theory for i = 1, ..., N charged electrons with a many-body Hamiltonian,

$$H = \sum_{i} \frac{\boldsymbol{p}_{i}^{2}}{2m} c_{i\sigma}^{\dagger} c_{i\sigma} + \sum_{i} U(\boldsymbol{r}_{i}) n(\boldsymbol{r}_{i}) + \frac{1}{2} \sum_{i \neq j} V(\boldsymbol{r}_{i} - \boldsymbol{r}_{j}) n(\boldsymbol{r}_{i}) n(\boldsymbol{r}_{j}), \quad (21)$$

where we have assumed a Galilean-invariant dispersion with bare mass, m, an onsite potential, $U(\mathbf{r}_i)$, and density-density interaction, $V(\mathbf{r}_i - \mathbf{r}_j)$. Computing the detailed ω dependence of $\sigma(\omega)$ for this theory can be quite complicated, as it depends on the many-body phase, which is determined by the hierarchy of energy scales, filling, and other parameters. However, if we are interested in the total integrated optical spectral weight \mathbb{S} , we can evaluate it simply by computing the double commutators in Eq. (20a), and we find $\mathbb{S} = \pi e^2 n/m$ (which is again related to T_F up to an overall prefactor). Note that the result here applies regardless of the specific many-body phase. This is simply the classic optical f-sum-rule [85]. The simplicity of the sum-rule stems partly from the purely local interaction terms V that do not couple to the external vector potential. We will return to this point shortly, as this formulation is not accurate for low-energy models of moiré materials.

While powerful and rigorous, the above statement is not necessarily "useful" in generic electronic solids, where the full optical spectral weight \mathbb{S} is O(eV) and thus bounds T_c by the same energy scale. In special situations with low electronic density where T_F is small, this can serve as a tight upper bound. More generally, the model can be deformed at the single-particle level, starting from a non-trivial bandstructure (instead of parabolic bands) while preserving interaction terms. The external probe gauge field still couples only to the kinetic energy piece, and the sum-rule can still be evaluated straightforwardly, though it appears more complicated [84]. However, since this sum-rule examines the entire spectral weight out to infinity and includes all "inter-band" transitions, the spectral weight remains O(eV). This prompts the question whether one can do better using partial sum-rules that extend over a lower range of energy scales to place tighter bounds on T_c [86, 87, 88, 89].

An ideal and non-trivial example of using partial sum-rules is provided by moiré systems, where one can potentially bound T_c in the absence of a microscopic mechanism for superconductivity. In the regime of interest, the physics is determined only by a subset of lowest energy bands, isolated from higher energy bands by a bandgap E_b and, as in MATBG; see Fig. 6. At a partial filling of low-energy bands, if interactions do

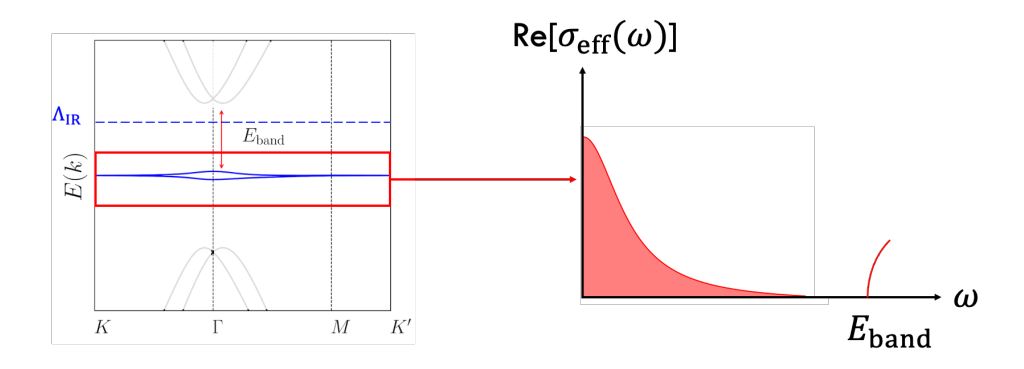


Figure 6. Restricted sum-rule, $\overline{\mathbb{S}} = \int_0^{\Lambda_{\rm IR}} \operatorname{Re}[\sigma_{\rm eff}(\omega)] d\omega$ associated only with the "intraband" transitions within the low-energy active bands.

not couple degrees of freedom across the gap $(V \ll E_{\rm band})$, we can ask for the analog of Eq. 20a when restricting attention to the low-energy theory up to frequency scale $_{\rm IR}$, i.e., $\overline{\mathbb{S}} = \int_0^{\Lambda_{\rm IR}} {\rm Re}[\sigma_{\rm eff}(\omega)] \ d\omega$. This leads to several interesting conceptual subtleties. First, integrated optical response associated only with low-energy theory should involve only low-energy degrees of freedom, but the microscopic current operator generically mixes low and high energy degrees of freedom. Second, once the interactions are projected to the low-energy theory in settings where the bands carry non-trivial quantum geometry, interactions need not remain local and can couple directly to the external vector potential. This is expected since interactions generate single-particle bandwidth and other interaction-induced terms (such as pair-hopping), which can couple directly to the external vector potential. Conceptually, given the projected low-energy effective theory $H_{\text{eff}} = \mathbb{P}H\mathbb{P}$, where \mathbb{P} is the projector to "active" bands (constructed from their Bloch wavefunctions [71]), how should one introduce minimal coupling to the low-energy degrees of freedom? Properly addressing these questions and carefully "integrating-out" the remote degrees of freedom requires using a Schrieffer-Wolff transformation [90, 87].

There is an elegant route that directly yields the correct expression for the partial sum-rule. Note that the double-commutator structure in Eq. (20a) can be rewritten as $\lim_{\alpha\to 0}\partial_{\alpha}^2 \mathrm{Tr}\left(\hat{\rho}e^{i\alpha\hat{X}}He^{-i\alpha\hat{X}}\right)$, which effectively encodes minimal coupling and computes the second-order response, $\delta^2 H/\delta A^2$, in the presence of an infinitesimal external vector potential. The form of the minimal coupling is fixed by the microscopic U(1) charge conservation tied to all of the electrons in the problem. In the projected limit, given an emergent U(1) conservation law associated with only the density in the active bands, the appropriate quantity to evaluate is $\lim_{\alpha\to 0}\partial_{\alpha}^2\mathrm{Tr}\left(\hat{\rho}e^{i\alpha\mathbb{P}\hat{X}\mathbb{P}}\mathbb{P}H\mathbb{P}e^{-i\alpha\mathbb{P}\hat{X}\mathbb{P}}\right)$, which yields

$$\overline{\mathbb{S}} = \int_0^{\Lambda_{\rm IR}} \operatorname{Re}[\sigma_{\rm eff}(\omega)] \ d\omega = -\frac{\pi}{2} \operatorname{Tr}\left(\hat{\rho}[\mathbb{P}\hat{X}\mathbb{P}, [\mathbb{P}\hat{X}\mathbb{P}, \mathbb{P}\hat{H}\mathbb{P}]]\right). \tag{22}$$

It can be explicitly verified that this addresses all of the previously raised subtleties about the low-energy response. However, while deceptively simple to write down, this expression is quite complicated to evaluate exactly for interacting theories since it also involves four-fermion expectation values [87] (for reasons explained previously). Nevertheless, there are several non-trivial and strongly interacting "solvable" limits where the partial sum-rule can be evaluated exactly [89], and has been used to place strong constraints on T_c for MATBG due to screened Coulomb interactions [91].

5. Outlook

These lectures have attempted to formulate general principles, explore non-trivial theoretical mechanisms, and raised open questions in the pursuit of unconventional transport and superconductivity in strongly correlated electron systems. The approach has relied partly on the possible existence of "quantum bounds", which serves two goals: venturing beyond classic textbook descriptions of Fermi liquids and their well-understood instabilities (e.g. to pairing) into uncharted territories of interacting quantum matter, and attempting to resolve specific puzzles inspired by experiments in quantum materials where a partial microscopic understanding enables possible resolution. The frontier of strongly correlated systems continues to reveal unexpected phenomena that challenge our fundamental understanding and promise exciting discoveries in quantum many-body physics.

Acknowledgments

I am grateful to my numerous collaborators for stimulating discussions related to the problems described here. They include: Erez Berg, Haoyu Guo, Johannes Hofmann, Steve Kivelson, Andrew Mackenzie, Dan Mao, Adam McRoberts, Juan-Felipe Mendez Valderrama, Roderich Moessner, Subir Sachdev, T. Senthil, Evyatar Tulipman, Xuepeng Wang and Elina Zhakina. This work has been supported in part by a NSF CAREER grant (DMR-2237522), a Sloan Research Fellowship and research funds provided by Cornell University.

- [1] Ziman J M 2001 Electrons and phonons: the theory of transport phenomena in solids (Oxford university press)
- [2] Emery V J and Kivelson S A 1995 Phys. Rev. Lett. **74** 3253–3256
- [3] Bruin J A N, Sakai H, Perry R S and Mackenzie A P 2013 Science 339 804
- [4] Drude P 1900 Annalen der Physik **306** 566–613
- [5] Armitage N P 2018 Electrodynamics of correlated electron systems (*Preprint* http://arxiv.org/abs/0908.1126:0908.1126)
- [6] Shi L Y, Tagay Z, Liang J, Duong K, Wu Y, Ronning F, Schlom D G, Shen K M and Armitage N P 2025 Phys. Rev. B 111(16) 165113 URL https://link.aps.org/doi/10.1103/PhysRevB. 111.165113
- [7] Hartnoll S A and Mackenzie A P 2022 Rev. Mod. Phys. 94 041002
- [8] Chowdhury D, Georges A, Parcollet O and Sachdev S 2022 Rev. Mod. Phys. 94 035004 ISSN 0034-6861, 1539-0756
- [9] Legros A, Benhabib S, Tabis W, Laliberté F, Dion M, Lizaire M, Vignolle B, Vignolles D, Raffy H, Li Z Z, Auban-Senzier P, Doiron-Leyraud N, Fournier P, Colson D, Taillefer L and Proust C 2018 Nature Physics 15 142–147 (Preprint http://arxiv.org/abs/1805.02512:1805.02512)
- [10] Cao Y, Chowdhury D, Rodan-Legrain D, Rubies-Bigorda O, Watanabe K, Taniguchi T, Senthil T and Jarillo-Herrero P 2020 Phys. Rev. Lett. 124 076801
- [11] Chen J H, Jang C, Xiao S, Ishigami M and Fuhrer M S 2008 Nature Nanotechnology 3 206 URL http://dx.doi.org/10.1038/nnano.2008.58
- [12] Efetov D K and Kim P 2010 Phys. Rev. Lett. 105 256805 ISSN 0031-9007, 1079-7114
- [13] Zaanen J 2004 Nature **430** 512–513
- [14] Sachdev S 1999 Quantum Phase Transitions 1st ed (Cambridge, UK: Cambridge University Press) URL http://www.cambridge.org/us/academic/subjects/physics/condensed-matter-physics-nanoscience-and-mesoscopic-physics/quantum-phase-transitions-2nd-edition?format=HB&isbn=9780521514682
- [15] Peierls E 1934 Zeitschrift für Physik 88 786-791 ISSN 0044-3328 URL https://doi.org/10. 1007/BF01333664
- [16] Giraldo-Gallo P, Galvis J A, Stegen Z, Modic K A, Balakirev F F, Betts J B, Lian X, Moir C, Riggs S C, Wu J, Bollinger A T, He X, Božović I, Ramshaw B J, McDonald R D, Boebinger G S and Shekhter A 2018 Science 361 479–481
- [17] Jaoui A, Das I, Di Battista G, Díez-Mérida J, Lu X, Watanabe K, Taniguchi T, Ishizuka H, Levitov L and Efetov D K 2022 Nat. Phys. 18 633–638 ISSN 1745-2481
- [18] Furrer A 1998 Neutron scattering in layered copper-oxide superconductors vol 20 (Springer Science & Business Media)
- [19] Koshino M and Son Y W 2019 Phys. Rev. B 100(7) 075416 URL https://link.aps.org/doi/ 10.1103/PhysRevB.100.075416
- [20] Mousatov C H and Hartnoll S A 2021 npj Quantum Mater. 6 1-6 ISSN 2397-4648
- [21] Chowdhury D, Werman Y, Berg E and Senthil T 2018 Phys. Rev. X 8 031024 (Preprint http://arxiv.org/abs/1801.06178:1801.06178)
- [22] Uemura Y J, Luke G M, Sternlieb B J, Brewer J H, Carolan J F, Hardy W N, Kadono R, Kempton J R, Kiefl R F, Kreitzman S R, Mulhern P, Riseman T M, Williams D L, Yang B X, Uchida S, Takagi H, Gopalakrishnan J, Sleight A W, Subramanian M A, Chien C L, Cieplak M Z, Xiao G, Lee V Y, Statt B W, Stronach C E, Kossler W J and Yu X H 1989 Phys. Rev. Lett. 62(19) 2317–2320
- [23] Cao Y, Fatemi V, Fang S, Watanabe K, Taniguchi T, Kaxiras E and Jarillo-Herrero P 2018 Nature 556 43–50
- [24] Leggett A J 1965 Phys. Rev. 140(6A) A1869-A1888 URL https://link.aps.org/doi/10.1103/ PhysRev.140.A1869
- [25] Landau L D 1957 Soviet Physics JETP 3 920-925 URL http://www.jetp.ras.ru/cgi-bin/e/index/e/3/6/p920?a=list

- [26] Abrikosov A Fundamentals of the Theory of Metals
- [27] Shankar R 1994 Rev. Mod. Phys. 66(1) 129-192 URL https://link.aps.org/doi/10.1103/ RevModPhys.66.129
- [28] Boltzmann L 1872 Wiener Berichte **66** 275–370
- [29] Prange R E and Kadanoff L P 1964 Phys. Rev. **134** A566–A580
- [30] Ahn S and Sarma S D 2022 Physical Review B 106
- [31] Aydin A, Keski-Rahkonen and Heller \mathbf{E} J 2024 Proceedings theNationalAcademySciences121 e2404853121(Preprint ofhttp://arxiv.org/abs/https://www.pnas.org/doi/pdf/10.1073/pnas.2404853121: https://www.pnas.org/doi/pdf/10.1073/pnas.2404853121) URL https://www.pnas.org/ doi/abs/10.1073/pnas.2404853121
- [32] Das Sarma S and Tu Y T 2024 Phys. Rev. B 109 235118 ISSN 2469-9950, 2469-9969
- [33] Paschen S and Si Q 2021 Nature Reviews Physics 3 9–26 ISSN 2522-5820 URL https://doi.org/ 10.1038/s42254-020-00262-6
- [34] Kubo R 1957 Journal of the Physical Society of Japan 12 570–586 (Preprint http://arxiv.org/abs/https://doi.org/10.1143/JPSJ.12.570: https://doi.org/10.1143/JPSJ.12.570) URL https://doi.org/10.1143/JPSJ.12.570
- [35] Mukerjee S, Oganesyan V and Huse D 2006 Phys. Rev. B 73 035113 (Preprint http://arxiv.org/abs/cond-mat/0503177:cond-mat/0503177)
- [36] Lindner N H and Auerbach A 2010 Phys. Rev. B 81(5) 054512 URL https://link.aps.org/doi/10.1103/PhysRevB.81.054512
- [37] Perepelitsky E, Galatas A, Mravlje J, Žitko R, Khatami E, Shastry B S and Georges A 2016 Phys. Rev. B 94(23) 235115 URL https://link.aps.org/doi/10.1103/PhysRevB.94.235115
- [38] Huang E W, Sheppard R, Moritz B and Devereaux T P 2019 Science 366 987–990 ISSN 0036-8075
- [39] Vranić A, Vučičević J, Kokalj J, Skolimowski J, Žitko R, Mravlje J and Tanasković D 2020 *Phys. Rev. B* **102**(11) 115142 URL https://link.aps.org/doi/10.1103/PhysRevB.102.115142
- [40] Vučičević J, Kokalj J, Žitko R, Wentzell N, Tanasković D and Mravlje J 2019 Phys. Rev. Lett. 123(3) 036601 URL https://link.aps.org/doi/10.1103/PhysRevLett.123.036601
- [41] Hartnoll S A 2015 Nature Phys 11 54-61 ISSN 1745-2481
- [42] Brown P T, Mitra D, Guardado-Sanchez E, Nourafkan R, Reymbaut A, Hébert C D, Bergeron S, Tremblay A M S, Kokalj J, Huse D A, Schauß P and Bakr W S 2019 Science **363** 379 (Preprint http://arxiv.org/abs/1802.09456:1802.09456)
- [43] Patel A A and Changlani H J 2022 Phys. Rev. B 105(20) L201108 URL https://link.aps.org/doi/10.1103/PhysRevB.105.L201108
- [44] Wannier G H 1950 Phys. Rev. 79(2) 357-364 URL https://link.aps.org/doi/10.1103/ PhysRev.79.357
- [45] Wannier G H 1973 Phys. Rev. B 7(11) 5017-5017 URL https://link.aps.org/doi/10.1103/ PhysRevB.7.5017
- [46] Stephenson J 1964 Journal of Mathematical Physics 5 1009–1024 URL https://doi.org/10. 1063/1.1704202
- [47] Houtappel R 1950 Physica 16 425 455 ISSN 0031-8914 URL http://www.sciencedirect.com/science/article/pii/0031891450901303
- [48] Melko R G, Paramekanti A, Burkov A A, Vishwanath A, Sheng D N and Balents L 2005 *Phys. Rev. Lett.* **95**(12) 127207 URL https://link.aps.org/doi/10.1103/PhysRevLett.95.127207
- [49] Heidarian D and Damle K 2005 Phys. Rev. Lett. 95(12) 127206 URL https://link.aps.org/doi/10.1103/PhysRevLett.95.127206
- [50] Wessel S and Troyer M 2005 Phys. Rev. Lett. 95(12) 127205 URL https://link.aps.org/doi/ 10.1103/PhysRevLett.95.127205
- [51] Mendez-Valderrama J F and Chowdhury D 2021 Phys. Rev. B 103(19) 195111 URL https://link.aps.org/doi/10.1103/PhysRevB.103.195111
- [52] Mousatov C H, Esterlis I and Hartnoll S A 2019 Phys. Rev. Lett. 122(18) 186601 URL https:

- //link.aps.org/doi/10.1103/PhysRevLett.122.186601
- [53] Sykes M F and Zucker I J 1961 Phys. Rev. 124(2) 410-414 URL https://link.aps.org/doi/ 10.1103/PhysRev.124.410
- [54] Fisher M E 1959 Phys. Rev. 113(4) 969-981 URL https://link.aps.org/doi/10.1103/ PhysRev.113.969
- [55] Park J M, Cao Y, Watanabe K, Taniguchi T and Jarillo-Herrero P 2021 Nature 592 43–48 ISSN 1476-4687 URL https://doi.org/10.1038/s41586-021-03366-w
- [56] Parcollet O and Georges A 1999 Phys. Rev. B 59 5341 (Preprint http://arxiv.org/abs/cond-mat/9806119:cond-mat/9806119)
- [57] Song X Y, Jian C M and Balents L 2017 Phys. Rev. Lett. 119 216601
- [58] Mackenzie A P 2017 Reports on Progress in Physics 80 032501 ISSN 0034-4885, 1361-6633 arXiv:1612.04948 [cond-mat] URL http://arxiv.org/abs/1612.04948
- [59] Hicks C W, Gibbs A S, Zhao L, Kushwaha P, Borrmann H, Mackenzie A P, Takatsu H, Yonezawa S, Maeno Y and Yelland E A 2015 Phys. Rev. B 92(1) 014425 URL https://link.aps.org/doi/10.1103/PhysRevB.92.014425
- [60] Mendez-Valderrama J F, Tulipman E, Zhakina E, Mackenzie A P, Berg E and Chowdhury D 2023 Proceedings of the National Academy of Sciences 120 e2305609120 (Preprint http://arxiv.org/abs/https://www.pnas.org/doi/pdf/10.1073/pnas.2305609120: https://www.pnas.org/doi/pdf/10.1073/pnas.2305609120) URL https://www.pnas.org/doi/abs/10.1073/pnas.2305609120
- [61] Zhakina E, Daou R, Maignan A, McGuinness P H, König M, Rosner H, Kim S J, Khim S, Grasset R, Konczykowski M, Tulipman E, Mendez-Valderrama J F, Chowdhury D, Berg E and Mackenzie A P 2023 Proceedings of the National Academy of Sciences 120 e2307334120 (Preprint http://arxiv.org/abs/https://www.pnas.org/doi/pdf/10.1073/pnas.2307334120: https://www.pnas.org/doi/pdf/10.1073/pnas.2307334120) URL https://www.pnas.org/doi/abs/10.1073/pnas.2307334120
- [62] Rullier-Albenque F, Alloul H and Tourbot R 2003 Phys. Rev. Lett. 91(4) 047001 URL https://link.aps.org/doi/10.1103/PhysRevLett.91.047001
- [63] Sunko V 2019 Angle Resolved Photoemission Spectroscopy of Delafossite Metals URL http://link.springer.com/10.1007/978-3-030-31087-5
- [64] Sunko V, Mazzola F, Kitamura S, Khim S, Kushwaha P, Clark O J, Watson M D, Marković I, Biswas D, Pourovskii L, Kim T K, Lee T L, Thakur P K, Rosner H, Georges A, Moessner R, Oka T, Mackenzie A P and King P D C 2020 Science Advances 6 eaaz0611 URL https://www.science.org/doi/10.1126/sciadv.aaz0611
- [65] McRoberts A J, Mendez-Valderrama J F, Moessner R and Chowdhury D 2023 Phys. Rev. B 107(2) L020402 URL https://link.aps.org/doi/10.1103/PhysRevB.107.L020402
- [66] Murthy C, Pandey A, Esterlis I and Kivelson S A 2023 Proceedings of the National Academy of Sciences 120 e2216241120
- [67] Nelson D R and Kosterlitz J M 1977 Phys. Rev. Lett. 39(19) 1201-1205 URL https://link.aps.org/doi/10.1103/PhysRevLett.39.1201
- [68] Becca F and Sorella S 2017 Quantum Monte Carlo approaches for correlated systems (Cambridge University Press)
- [69] Paiva T, Scalettar R, Randeria M and Trivedi N 2010 Phys. Rev. Lett. 104(6) 066406 URL https://link.aps.org/doi/10.1103/PhysRevLett.104.066406
- [70] Hofmann J S, Chowdhury D, Kivelson S A and Berg E 2022 npj Quantum Materials 7 83 ISSN 2397-4648 URL https://doi.org/10.1038/s41535-022-00491-1
- [71] Marzari N, Mostofi A A, Yates J R, Souza I and Vanderbilt D 2012 Rev. Mod. Phys. 84(4) 1419–1475 URL https://link.aps.org/doi/10.1103/RevModPhys.84.1419
- [72] Törmä P, Peotta S and Bernevig B A 2022 Nature Reviews Physics 4 528–542 ISSN 2522-5820 URL https://doi.org/10.1038/s42254-022-00466-y
- [73] Hofmann J S, Berg E and Chowdhury D 2020 Phys. Rev. B 102(20) 201112 URL https:

- //link.aps.org/doi/10.1103/PhysRevB.102.201112
- [74] Zhang X, Sun K, Li H, Pan G and Meng Z Y 2022 Phys. Rev. B 106(18) 184517 URL https://link.aps.org/doi/10.1103/PhysRevB.106.184517
- [75] Peri V, Song Z D, Bernevig B A and Huber S D 2021 Phys. Rev. Lett. 126(2) 027002 URL https://link.aps.org/doi/10.1103/PhysRevLett.126.027002
- [76] Herzog-Arbeitman J, Peri V, Schindler F, Huber S D and Bernevig B A 2022 Physical Review Letters 128 087002 ISSN 0031-9007 URL https://link.aps.org/doi/10.1103/PhysRevLett. 128.087002
- [77] Hofmann J S, Berg E and Chowdhury D 2023 Phys. Rev. Lett. 130(22) 226001 URL https://link.aps.org/doi/10.1103/PhysRevLett.130.226001
- [78] Emery V J and Kivelson S A 1995 Nature 374 434–437 ISSN 1476-4687
- [79] Orenstein J, Thomas G A, Millis A J, Cooper S L, Rapkine D H, Timusk T, Schneemeyer L F and Waszczak J V 1990 Phys. Rev. B 42(10) 6342-6362 URL https://link.aps.org/doi/10.1103/PhysRevB.42.6342
- [80] Nachumi B, Keren A, Kojima K, Larkin M, Luke G M, Merrin J, Tchernyshöv O, Uemura Y J, Ichikawa N, Goto M and Uchida S 1996 Phys. Rev. Lett. 77(27) 5421-5424 URL https://link.aps.org/doi/10.1103/PhysRevLett.77.5421
- [81] Popov V N 1972 Theor. Math. Phys. 11 354–365
- [82] Kagan Y, Svistunov B and Shlyapnikov G 1987 Sov. Phys. JETP 66 314–323
- [83] Fisher D S and Hohenberg P C 1988 Phys. Rev. B 37(10) 4936–4943
- [84] Hazra T, Verma N and Randeria M 2019 Physical Review X 9 031049
- [85] Pines D 2018 Elementary excitations in solids (CRC Press)
- [86] Millis A J 2004 Optical conductivity and correlated electron physics (Dordrecht: Springer Netherlands) pp 195–235 ISBN 978-1-4020-3463-3 URL https://doi.org/10.1007/978-1-4020-3463-3_7
- [87] Mao D and Chowdhury D 2023 Proceedings of the National Academy of Sciences 120 e2217816120 URL https://www.pnas.org/doi/abs/10.1073/pnas.2217816120
- [88] Verma N, Hazra T and Randeria M 2021 Proceedings of the National Academy of Sciences 118 e2106744118
- [89] Mao D and Chowdhury D 2024 Phys. Rev. B 109(2) 024507 URL https://link.aps.org/doi/ 10.1103/PhysRevB.109.024507
- [90] Sondhi S and Kivelson S 1992 Physical Review B 46 13319
- [91] Mendez-Valderrama J F, Mao D and Chowdhury D 2024 Phys. Rev. Lett. 133(19) 196501 URL https://link.aps.org/doi/10.1103/PhysRevLett.133.196501